Modeling of Mechanical Alloying: Part III. Applications of Computational Programs

D. MAURICE and T.H. COURTNEY

The computational modeling programs described in part II of this series are used in two ways. One is to compare program predictions to previous experimental data, thereby testing to some extent the utility of the programs. At this stage of their development, program "predictions" with respect to processing time, microstructural scale, and similar parameters are accurate to within a factor of 2 or so. Even so, the predictions offer support of the model developed in part I of this series and provide a vehicle for both model and process refinements. In addition to "testing" the model and the program in these manners, the effect of uncertainty in input material properties on program predictions is explored.

I. INTRODUCTION

IN the first two parts of this series,[1,2] we established a protocol for specifying the occurrences of deformation, coalescence, and fragmentation events endemic to mechanical alloying (MA) and mechanical milling (MM), and we outlined development of a computational algorithm which simulates the temporal evolution of powder during these processes. In this, the final installment of the series, we examine the capabilities of our model by comparing predictions of it to published studies. The predictions use "first guess" data with regard to input of material properties and process variables. While we find the resulting predictions are not as accurate as they might be (typically, they are within a factor of 2 or so with respect to experimentally observed processing times, particle sizes, *etc.*), they do indicate the usefulness of the model documented in this series. We also investigate the effect that uncertainties in powder property data have on model predictions. This is important for, among other reasons, property data are usually derived from bulk material and not from the powder being used during MA and MM.

II. APPLICATIONS

A. *Mechanical Alloying of Iron-Chromium in a SPEX Mill*

Benjamin and Volin[3] observed five stages of powder evolution during MA of two-phase Fe-Cr alloys in a SPEX (SPEX Industries, Edison, NJ) mill (Figure 1). The first—particle flattening—results from plastic deformation. Particle welding, with the average particle size increasing, follows. A subsequent stage is referred to as "equiaxed particle formation;" welding and fracture events take place at approximately the same rate during this stage, and phase lamellae within individual particles remain more or less parallel to each other. The fourth stage is called random welding orientation; fracture and welding frequencies are still primarily in balance here, but a number of randomly oriented lamellar "colonies" exist within individual particles. During the fifth and final stage, "steady state processing," particle microstructural refinement continues though size remains approximately constant. This study of Benjamin and Volin is especially relevant for comparison with model predictions, as the trends noted by them are almost universally found during MA of systems composed of malleable powders. In this section, we show that the programs described essentially predict these stages and their approximate duration and (also approximately) the measured powder characteristics (hardness, size, and lamellar thickness). Process parameters and material property data used in the programs are provided in Tables I and II, respectively.

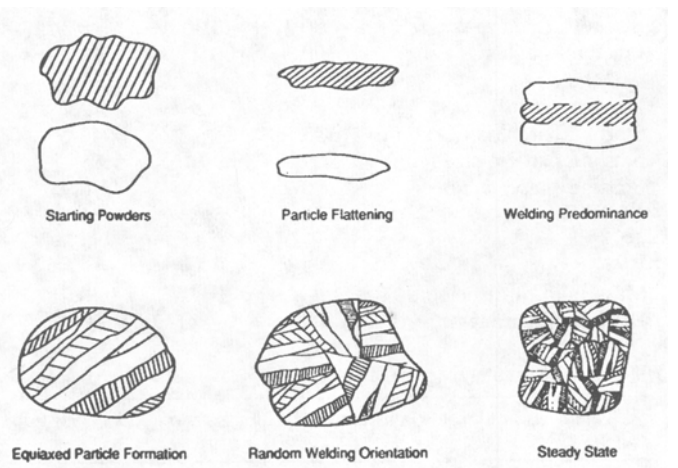

Fig. 1—The five stages of powder evolution during MA.[3] Particle flattening (the first stage) results from plastic deformation. This is followed by a welding dominance stage during which the average particle size increases. During the third stage (equiaxed particle formation), welding and fracturing are rather much in balance and phase lamellae within individual particles are more-or-less parallel. Random welding orientation is the fourth stage. Fracture and welding tendencies are still in balance, but a number of lamellar colonies exist within each particle. Steady-state processing, during which microstructural refinement continues, constitutes the final stage.

D. MAURICE, formerly Graduate Student, Department of Materials Science and Engineering, University of Virginia, Charlottesville, VA 22903, is NRC Research Associate, Albany Research Center, U.S. Bureau of Mines, Albany, OR 97321. T.H. COURTNEY, formerly Professor, Department of Materials Science and Engineering, University of Virginia, is Professor and Chair, Department of Metallurgical and Materials Engineering, Michigan Technological University, Houghton, MI 49931.

Manuscript submitted June 17, 1994.

Table I. Process Parameters Used in Applications of Model

Process Parameter	Fe-Cr (MAP2)	Al (MAP1)
Ball diameter (mm)	7.9	6.35
Ball density (g/cm³)	7.8	7.8
Charge ratio	5.9	6.3
h_0 (μm)	100	100
Impact angle (deg)	0	0
Impact velocity (m/s)	4.0	4.0
Impact frequency (s^{-1})	7.28	7.28

Table II. Material Property Data Used in Applications of Model

	Fe-Cr (MAP2)		Al (MAP1)
Property	Fe	Cr	—
Modulus (GPa)	200	250	72
Tensile strength (MPa)	303	290	90
Strain to fracture	0.37	0.30	0.34
Fracture toughness (MPa$\sqrt{m}$)	100	100	20
Density (g/cm³)	7.8	7.2	2.7
Starting hardness (kg_f/mm^2)	125	125	40
Starting particle size (μm)	89	89	75
Starting shape factor	0.95	0.50	0.95
K^* (MPa)	175	175	104
n^*	1.0	1.0	0.37
Weight fraction	0.52	0.48	—
Mass ratio of dispersoid	—	—	0, 0.01
Dispersoid hardness (kg_f/mm^2)	—	—	550
Dispersoid diameter (μm)	—	—	0.1

*Parameter used in the constitutive equation $\sigma = \sigma_O + K\varepsilon^n$ and for which $H_v = 3\sigma$.

Particle flattening produces a decrease in the particle shape factor, f_s. During this stage, particles become platelike. Welding also commences, leading to development of the characteristic lamellar structure of processed powders. Benjamin and Volin[3] found this period lasted for the first 12 minutes of milling. In our model, f_s is predicted to decrease during the first 10 to 12 minutes of milling (Figure 2).

The period of welding predominance is the time frame over which the welding rate exceeds the fracture rate. Benjamin and Volin[3] found this period to lie between ca. 12 to 30 minutes of processing; Figure 3 shows that the model predicts welding to dominate fracture for the first 12 minutes of processing. Particle size increases during the stage of welding dominance. Model predictions (Figure 4) indicate that a maximum in particle size should be found after about 12 minutes of processing; empirically, the maximum size is found after 30 minutes. The measured maximum average particle size is about 100 μm, while the predicted size is about 130 μm. (We should note here that the programs in their current form do not handle size distributions; thus, the empirically determined 50th percentile is taken as a basis for comparison.)

An increase in f_s is concurrent with equiaxed particle formation. During this stage, weld and fracture events (which increase f_s) take place at a reasonable frequency (Figure 3), while the deformation per impact (which reduces f_s) is diminished due to the powder's greater hardness. Experimentally, this period lasted roughly through 30 to 60 minutes of milling. MAP2 predicts this period should extend from ca. 12 to 40 minutes (Figure 2).

Random welding orientation was found to commence after milling for about 1 hour. As welds tend to be oriented parallel to the grinding media surfaces, the orientation of

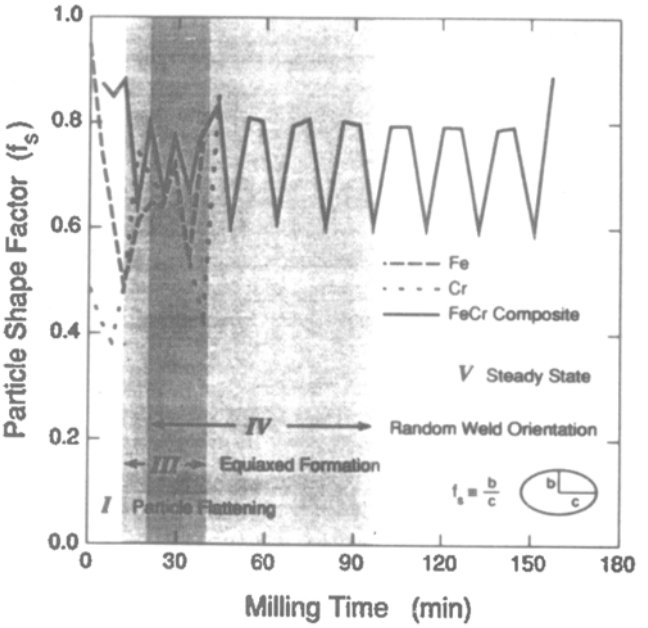

Fig. 2—Three of the five stages of microstructural evolution are predicted by simulation of the particle shape factor, f_s. Stage I (particle flattening) results in a reduction in f_s. Stage III, equiaxed particle formation, results in an increase in f_s. Random weld orientation (stage IV) is reflected by repeated reversals in f_s. The predicted final (steady-state) stage corresponds to an approximately constant value of f_s. In addition, particle size and lamellar thickness change gradually with processing time during steady-state processing (Figures 4 and 5).

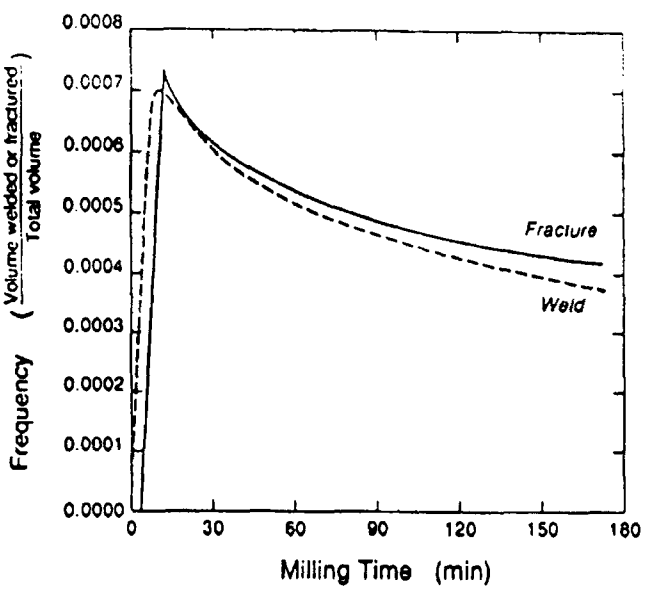

Fig. 3—Weld and fracture frequencies for the Fe-Cr system. Computed frequencies are expressed as volume welded (fractured) during an impact divided by the total volume of powder associated with each ball. Weld frequencies exceed the corresponding fracture ones for the first 12 min of processing. This is accompanied by an increase in average particle size. For process times longer than 12 min, the opposite holds.

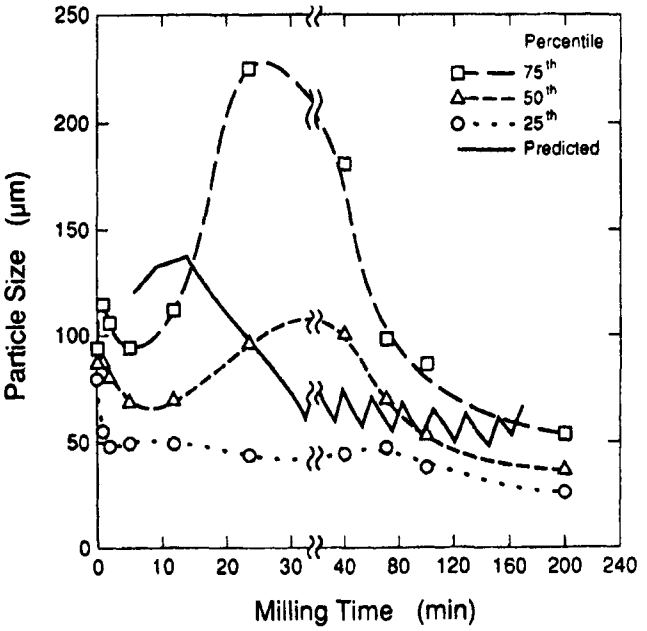

Fig. 4—Measured particle size[3] for SPEX milled Fe-Cr alloys and average particle size as predicted by MAP2. The latter size should be compared to the experimental 50th percentile curve. MAP2 predicts a slightly larger maximum average particle size, which should be observed after 12 min of processing. The maximum average size is experimentally observed after about 30 min. Steady state also commences earlier according to MAP2, but measured and predicted steady-state particle sizes are about the same.

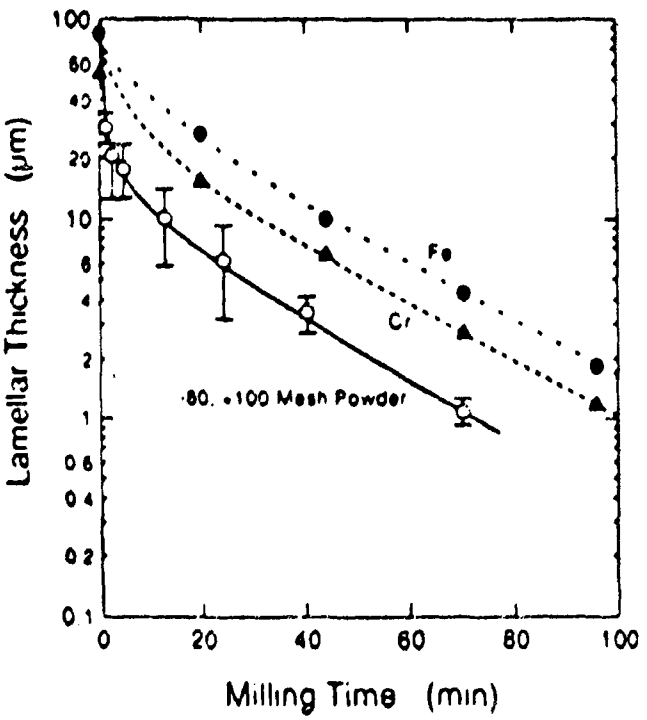

Fig. 5—Measured (open circles) and predicted (filled symbols) lamellar thicknesses for SPEX milled Fe-Cr alloys. MAP2 predicts a coarser microstructure than is observed. This, along with the hardness data of Figure 6, indicates MAP2 underestimates powder deformation per impact.

the particles on the ball surfaces determines the placement of newly welded lamellae. When the alignment of the particles on the balls reverses, so does that of the subsequently welded lamellae. In our description, this corresponds to re-

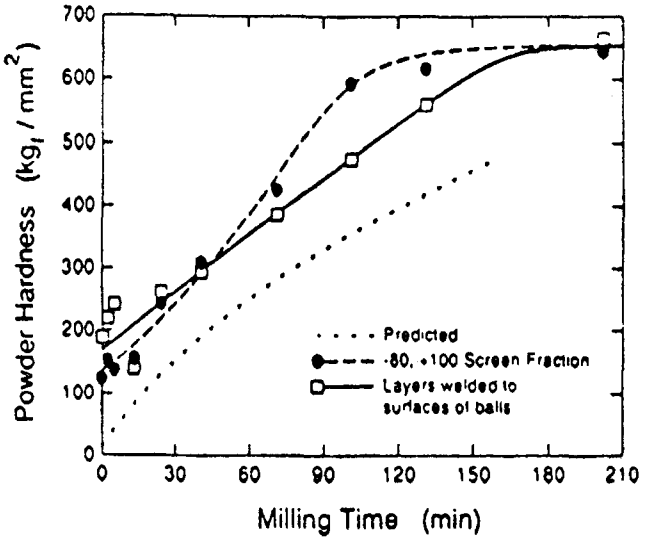

Fig. 6—Measured and predicted powder hardnesses for SPEX milled Fe-Cr alloys. Although the trend in hardness predicted by MAP2 is consistent with that observed, predicted hardnesses are lower. This also suggests deformation per impact is underestimated with MAP2.

petitive reversals in f_s; the program representation of this description predicts this to happen after approximately 25 minutes of milling (Figure 2).

Average particle size remains approximately constant (ca. 50 μm, Figure 4) in the final, "steady" state; the program predicted average size during steady state is about 60 μm. Because of the greater powder hardness in this stage, deformation per impact is less and weld and fracture frequencies are also reduced. Steady state commences after about 100 minutes of processing; Figure 4 shows the model predicted size remains essentially constant after about 40 minutes (on the model, this corresponds to the onset of steady state).

While model predictions, with respect to the processing stages and the variations in particle size, are in qualitative to semiquantitative accord with experimental observations, there is a systematic error in the corresponding process times by a factor of about 2.5. This points to an overestimate of the effective impact frequency, which can be corrected for in the programs if desired. Errors in estimation of impact frequency and velocity stem from imperfect mating of local and global modeling. Powder is in fact subjected to a distribution of impact velocities and frequencies; global studies[4–7] have demonstrated their range may be quite large. However, in order to minimize programming complexity, our programs rely upon the repetition of a single characteristic and effective impact. Incorporation of the actual distributions could well result in quite different times for the various stages and perhaps somewhat different values for the powder variables, although the trends predicted should be only minimally affected.

Comparison of predicted and experimentally observed microstructural refinement can also be made. After 40 minutes of milling, Benjamin and Volin[3] found an average lamellar thickness of 2.85 μm (Figure 5); the model predicted corresponding thickness should be about 10 μm. This discrepancy is mirrored by differences between predicted and measured hardnesses. As shown in Figure 6, the hardness measured after 40 minutes of milling is 308

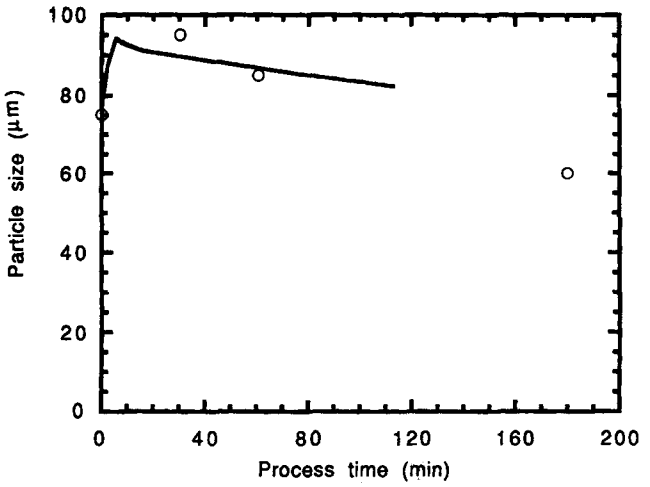

Fig. 7—Measured (open circles[12]) and MAP1 predicted (solid line) median particle sizes for SPEX milled Al. There is good agreement between predictions and experimental results, both with respect to maximum median particle size and the time evolution of the median size. A caveat is given in the text.

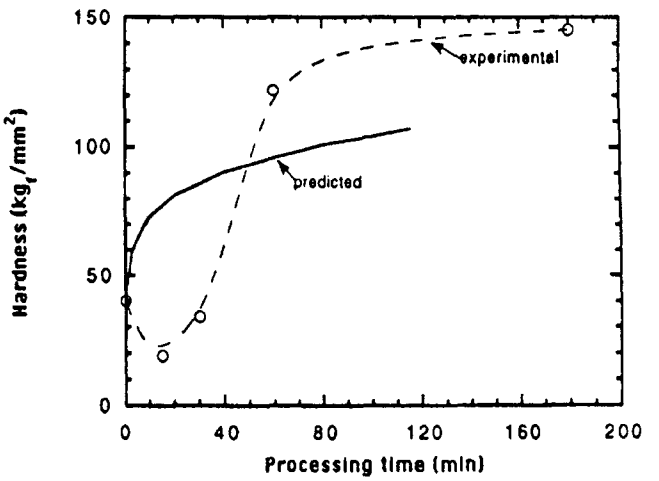

Fig. 8—Predicted and measured[12] microhardnesses of SPEX milled Al. Predicted hardnesses are about 20 pct less than measured ones at longer processing times.

kg/mm^2; the corresponding predicted hardness is only 235 kg/mm^2. Both discrepancies indicate that the predicted powder deformation per impact is less than that occurring. Correction in this case suggests adjustment of the constitutive deformation laws of the powder constituents. Complicating such an adjustment, though, is the well-established fact that two-phase materials work harden more rapidly than do single-phase ones, especially at large deformation strains. This makes the representation of adequate constitutive laws difficult, in that the law for the composite particles can no longer be obtained by suitably averaging the corresponding laws for the composite constituents.*

*Temperature may also play a role here, although we do not believe it to be a major one. Several studies[8,9,10] have attempted to estimate powder temperature increases as a result of ball-powder-ball collisions. Such temperature increases are modest for the most part but can be as high as several hundred kelvin in an energetic mill. Beyond that, the temperature decreases rapidly (within a time estimated to be on the order of 10^{-2} s) to the ambient mill temperature,[9] so it is unlikely significant material recovery occurs in the interim. And certainly, the times and temperature of heating are insufficient to induce morphological changes in the powders.[11]

In summary, MAP2 apparently overestimates the collision frequency and underestimates the deformation a particle experiences in a collision. However, given the complexity of the process, not to mention the approximations made in the model development and the uncertainty in the material properties used, the program demonstrates reasonable predictive powers.

B. *Mechanical Alloying of Aluminum in a SPEX Mill*

Gilman and Nix[12] mechanically alloyed Al powder in a SPEX mill. The essentially single-phase nature of this system allows the use of MAP1 for predictive purposes. Our comparisons with Gilman and Nix's results are of necessity limited to particle size and hardness. (Tables I and II show the process parameters and material property data used in the computations.)

Figure 7 shows that the experimentally determined median particle size increased rapidly to nearly 100 μm during the initial processing stage. Model predictions also indicate a rapid initial increase in size to 94 μm. This suggests frequent welding in the early processing stages, as reported.[12] After 1 hour of processing, the experimentally measured and predicted median particle size are both on the order of 85 μm. Apparently, here there is good agreement between prediction and experiment. However, in order to prevent excessive cold welding of Al, Gilman and Nix were forced to use a process control agent (PCA) in their work. Our program considered milling of pure Al absent a PCA. Thus, we conclude that pure Al welds more rapidly than our model predicts. As described later, though, the model is capable of qualitatively describing the delay in particle welding when PCAs are employed.

Predicted and experimental microhardnesses may also be compared, as in Figure 8. Experimentally determined hardnesses are 120 and 140 kg/mm^2 after milling for 1 and 3 hours, respectively. Predicted hardnesses are 95 kg/mm^2 and (by extrapolation) 120 kg/mm^2. Agreement is reasonable; the model-underestimated hardnesses are similar to what is found with the Fe-Cr alloys.

It is notable that model predictions for this system more closely match experimental data than did those for the Fe-Cr system. This could be a result of systematic error in the property data set used for Fe-Cr or to factors overlooked in modeling. As noted earlier, predicted hardnesses are less than measured ones for both systems. This could result from deficiencies in the constitutive relationships utilized, from underestimation of impact velocity, or from overestimation of powder coating thickness. Increasing impact velocity results in a reduction in the interval between impacts, while decreasing coating thickness increases this interval[11] (although the deformation per impact increases with decreases in h_o).

In light of the uncertainty in many of the variables used in computational modeling, the possibility of empirically fixing a "time constant" for each system is not unreasonable as a means for model refinement, thereby rendering it more practically useful. Once established for a specific system, no additional parameter adjustments ought to be required as experimental and predicted trends in properties, particle size, *etc.* are in accord.

We close this section on MA processing of Al by discussion of the effect dispersoids have on processing. In addition to strengthening product alloys, dispersoids may function as PCAs. Their presence between ductile particles inhibits welding by reducing metal-metal contact area and by providing an elastic recovery force.[1] A familiar combination is Al with Al_2O_3. As experimental (and model) studies show, pure Al is predisposed to weld readily in the early milling stages, resulting in a rapid increase in particle size. If 1 wt pct of Al_2O_3 particles of 0.1-μm diameter is added to Al, the model (using MAP1) predicts onset of particle welding in a SPEX mill to be delayed for nearly 20 minutes relative to that of pure Al (Figure 9(a)); this results in a particle size finer than that of the starting powders (Figure 9(b)). Model predictions are in accord with generally observed trends for milling Al with Al_2O_3 or organic PCAs, but insufficient data are available to make detailed comparisons.

III. PROCESSING KINETICS AS RELATED TO, AND PROGRAM SENSITIVITY OF, MATERIAL PROPERTIES

The usefulness of computational programs for describing complex material processes often lies more in the ability to identify key process variables than in quantitative predictive capabilities. In this section, we apply the model in such a way. It is used to describe the kinetics of alloy particle formation, and some resultant powder characteristics, as they are affected by differences in initial properties of the alloy constituents. In another article[13] dealing with global aspects of MA/MM, we discuss how process variables (*e.g.*, impact velocity) and material property variations influence alloy particle formation. Here, though, we focus on how program predictions change when reasonable alterations in the material property data set are made. The system investigated is the previously described Fe-Cr one. The results obtained reinforce ideas noted previously with respect to over reliance on "absolute values" of program predictions. On the other hand, the results also suggest means for empirical refinement of the programs so as to make them more quantitatively accurate.

There are some staunch, current efforts to develop reliable material property data bases.[14,15] Most such compilations, though, remain incomplete. In addition, properties of pure elements are (sometimes strongly) sensitive to their purity level, mode of manufacture, and other factors (*e.g.*, whether the material is cold worked or recrystallized). Powder materials are even more difficult to contend with in this respect. They are made in many different (often unspecified by the supplier) ways. Additionally, powders typically have interstitial contents considerably higher than their wrought or cast counterparts.

As noted in Section II, educated "guesses" were made for many of the material properties used in the programs; primary sources used for this purpose were References 16 and 17. With regard to the initial Fe-Cr data set, we also employed the following procedure. The interlamellar spacing found by Benjamin and Volin was used to estimate the powder strain per unit time. Knowing this and the initial value, and time variation, of the powder hardness permitted determination of the parameters in the plastic constitutive

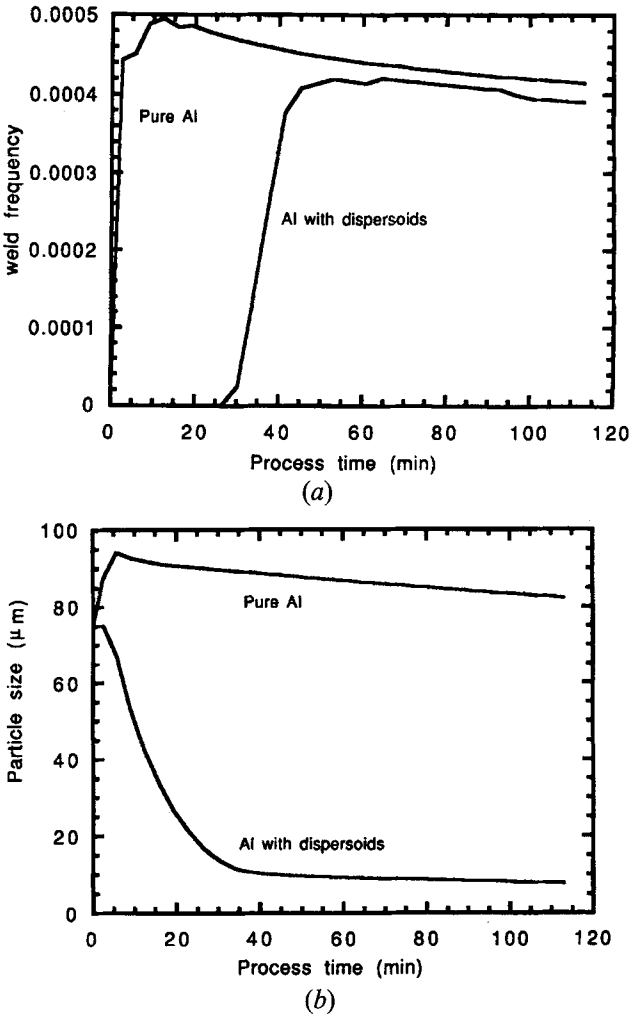

Fig. 9—The effect of alumina dispersoids on the MA characteristics of Al, as predicted by MAP1. (*a*) Adding 1 wt pct dispersoid delays welding for about 25 min (units for weld frequency are the same as in Fig. 3). (*b*) This results in a decrease in processed particle size.

equation for the composite species. Two aspects of this procedure should be noted. One is that we assumed the constitutive law for the alloy particle is the same as that for Fe, the softer of the alloy constituents. This does not much affect program results (recall a tenet of the model is that the harder species does not deform until the hardness of the initially softer species reaches that of the harder one). A second aspect is that, by virtue of using these procedures, we conclude that resultant "errors" in hardness predictions emanate from errors in estimated collision frequency and/or strain per collision. If either or both of these parameters are in error, no matter how accurate the constitutive laws used may be, the hardness predictions will not be accurate.

Other material properties used in the original data set for Fe-Cr were estimated from References 16 and 17. Chromium, though, is worrisome in this respect. Polycrystalline Cr is brittle at room temperature. Some Cr properties (*e.g.*, tensile strength and fracture initiation strain) were estimated from its tensile behavior at 673 K. These properties may be irrelevant to room temperature behavior, though we note Cr manifests significant ductility when it is mechanically alloyed with ductile constituents (*e.g.* Fe or Cu). Even allowing for this, the value of K_{Ic} assigned to it initially (*cf.* Table II) seems high. To assess the sensitivity of model

Table III. Fe-Cr Material Property Data Sets Used in MAP2

Data Set	TS (MPa)		Fracture Strain		K_{Ic} (MPa$\sqrt{m}$)		H_v (kg_f/mm^2)		K^* (MPa)		n^*	
	Fe	Cr	Fe	Cr	Fe	Cr	Fe	Cr	Fe	Cr	Fe	Cr
Original	303	290	0.37	0.30	100	100	125	125	175	175	1.0	1.0
1	500	400	0.412	0.10	100	30	90	110	500	400	1.0	1.0
1A	500	400	0.31	0.20	78	52	90	110	500	400	1.0	1.0
2	500	500	0.412	0.28	100	50	90	110	500	500	1.0	1.0
2A	500	500	0.412	0.28	90	60	90	110	500	500	1.0	1.0

*Parameters in the constitutive equation $\sigma = \sigma_0 + K\varepsilon^n$ and for which $H_v = 3\sigma$.

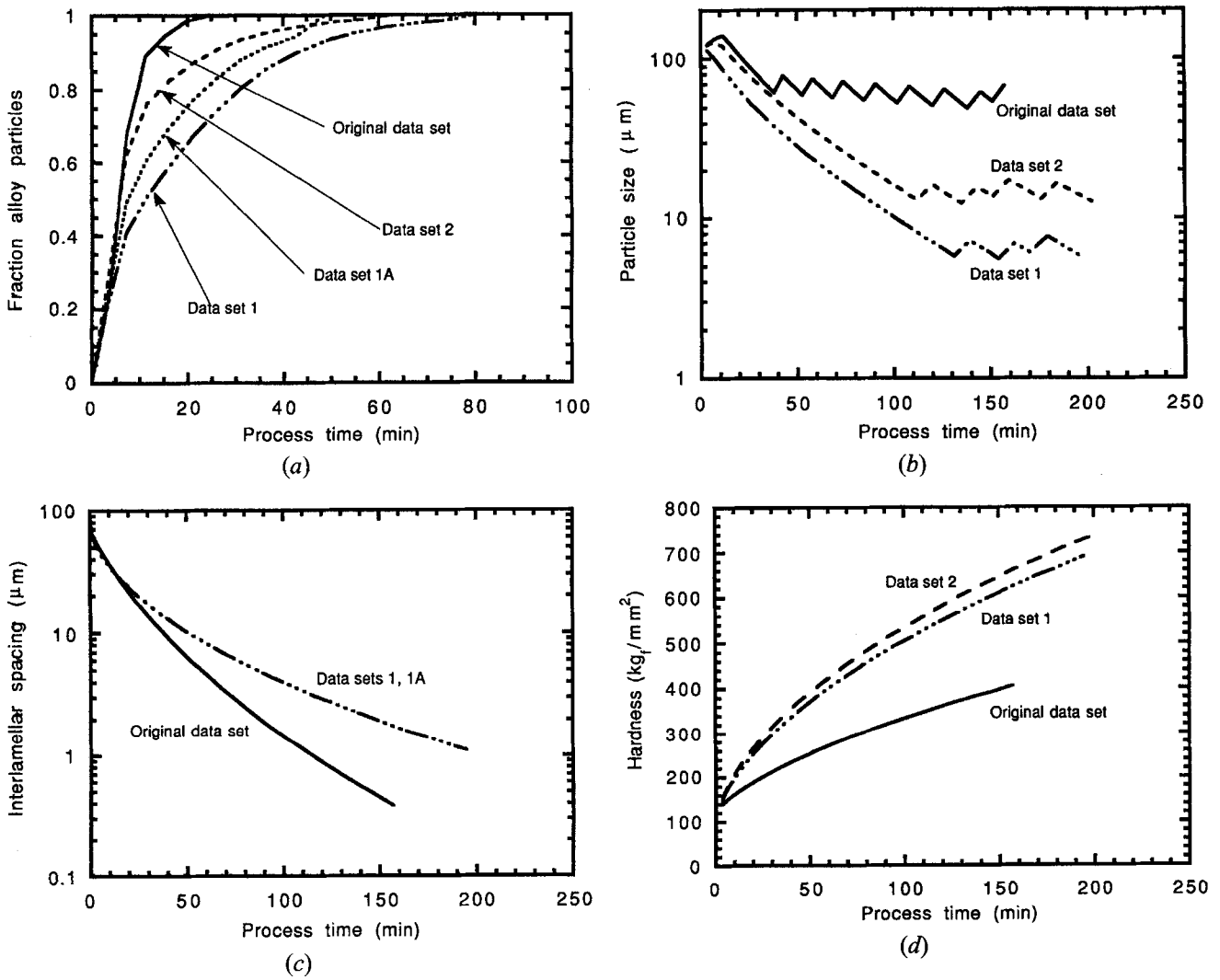

Fig. 10—The effect of varying material properties on (*a*) alloying kinetics, (*b*) processed particle size, (*c*) interlamellar spacing within particles, and (*d*) powder hardness. Alloying kinetics are reduced on using data sets different from the original one (alloying kinetics are essentially the same for data sets 2 and 2A), primarily as a result of the lower Cr fracture toughnessess used in the later data sets. This also results in a reduction in size of the processed powders. (Particle sizes for data sets 1A and 2A are very nearly the same as for data set 2.) Because of the higher hardening rates incorporated in the additional data sets, interlamellar spacings increase (c) and predicted hardnesses are higher (d). (Interlamellar spacings are the same for data sets 2 and 2A and are very close to those predicted on using data set 1. Predicted hardnesses are the same for data sets 2 and 2a and are also the same for data sets 1 and 1A.)

predictions to variations in property input data, different property data sets were used in MAP2 (Table III). The values of tensile strength and work-hardening characteristics in the additional data sets are consistent with what is known of the behavior of highly deformed Fe. Since other bcc refractory metals behave somewhat similarly, comparable alterations in Cr properties were made.

Results of using these different property data on program predictions are provided in Figures 10(a) through (d) and encapsulated in Table IV, where they can be compared to predictions obtained with the original data set. Other than for the different constitutive equations used, data set 1 is distinguished from the original set primarily by the lower values of fracture initiation strain and K_{Ic} for Cr (the value

Table IV. Process/Powder Characteristics as Dependent on Material Property Data Set

Data Set	Alloying Time (Min)	Particle Size (μm)/(at Time) (Min))	Particle Size (μm) at 2.5 h	H_v (kg_f/mm^2) at 2.5 h	Average Lamellar Spacing (μm) at 1 h
Original	16	134/11	55	397	4.7
1	54	91/3	6	609	8.3
1A	44	97/7	21	609	8.3
2	36	114/7	14	645	8.6
2A	35	115/7	21	645	8.6

of K_{Ic} for Cr in data set 1 is approximately that of a low toughness metal). Alloying time (the time needed to produce a powder population that is almost exclusively composite particles) is increased substantially with data set 1 (particle fracture earlier in the process generally increases alloying time), and particle size is significantly finer throughout processing. Predicted powder hardnesses are in good agreement with experimental ones, but this is somewhat misleading. That is, the constitutive law for data set 1 predicts significant hardening per unit strain. As a result, even though the hardnesses predicted with this data set are in accord with empirical ones, the predicted interlamellar spacings are much larger than the empirical ones. Data set 1A differs from data set 1 in that while the *average* fracture initiation strains and fracture toughnesses are the same in both sets, these properties are lower for Fe, and higher for Cr, in data set 1A. Alloying time is reduced thereby and average particle size is increased.

The Cr toughness and ductility are greater in data set 2 than in data set 1. This results in a reduction in alloying time and an increase in particle size. Average fracture toughnesses are the same in data sets 2 and 2A, but Cr toughness is higher and Fe toughness is lower for data set 2A. This results in a somewhat larger particle size during processing. Since the constitutive laws are similar for the additional data sets, program predicted hardnesses and interlamellar spacings are likewise similar.

All of these data sets (and undoubtedly others) are "reasonable" guesses. We note that powder properties and characteristics vary similarly with processing time for all data sets employed here. In a sense, this provides support for the physics underlying the model. However, the results shown here also realistically reflect limitations imposed by the uncertainties in material property data on the accuracy of program predictions. In this regard, optimum empirical use of the programs might be obtained as follows. Data (particle size, hardness, extent of alloy particle formation, and interlamellar spacing) could be obtained for a limited number of process times. A linear regression analysis, using program input parameters as variables, could be carried out and the "best fit" values for the parameters determined. Since the processing and property trends observed are well reflected by program predictions, these "empirical parameters" could be used with reasonable confidence for extrapolative purposes.

V. SUMMARY

In this article, we have compared computational predictions, based on a model of MA and its extension *via* numerical programs, to experimental results. The programs predict powder hardness and particle size, shape, and lamellar thickness changes during MA and MM of ductile species. Agreement of model predictions with experimental ones is reasonable, particularly in view of the large number of parameters which affect the process and because the predictions are based on guesses of material properties and process characteristics and, hence, adjustable parameters have not been employed. (Doing so would surely permit more accurate modeling.) The benefits of these predictions are twofold. First, they provide some support for the model, thereby giving insight into the possible actual "happenings" of MA. Second, by refinement and calibration of the myriad aspects of the model, they suggest a vehicle for establishing control over the dimensions and properties of output powders, thus possibly leading to more efficient processing routes.

Several model and algorithm refinements could enhance the versatility of the programs. Elaboration of the description of the mechanical response of balls coated with powder[1] would expand the range of impact velocities and coating thicknesses that the programs can handle and would allow for the possibility of the powder being harder than the grinding media. As a corollary, welding of powders to the media could be incorporated. In addition, MAP2 should be expanded to test for coalescence by particle encapsulation and for any transition between encapsulation and cold welding (the latter as defined in Reference 1). Programs could also be expanded to appraise the influence of mill atmosphere, as we have done in a work relating to nickel sulfide synthesis by MA.[18] The effect of mill atmosphere could be translated into a general consideration of the effect PCAs have on processing kinetics. Finally, the programs could be expanded to consider distributions in particle sizes, hardnesses, *etc.*, rather than just the average of these parameters as they do in their current form.

The model described in this series of articles is primarily a demonstration of possibility. It is limited by virtue of the stochastic nature and complexity of the process it attempts to describe and by the precision of the data upon which it relies. Nonetheless, it succeeds in predicting trends in powder morphological development and properties during milling of ductile metals. It also offers a reasonable framework for theoretical and empirical refinement.

APPENDIX
Access to MAP2

The MAP2 program package is available by electronic transfer. Those with access to Internet can obtain a copy *via* remote ftp. To do so, follow this procedure:

connect to ftp.mm.mtu.edu

at the log in prompt, type ftp

password: provide your full e-mail address (*e.g.*, thc @mtu.edu)

You will be informed that you have successfully logged in. At this point, type in

cd pub

Take the MAP2 file by the command

get MAP2.README

get MAP2.tar

This will put the files in your computer. The README file gives instructions for setting up the programs. A tutorial file found in the MAP2.tar package gives specific instructions for running the program. A tar file is an archive containing one or more other files in a convenient package. Use "tar xf MAP2.tar" to extract those files from this archive.

ACKNOWLEDGMENTS

The authors would like to thank Rosser L. Wayland III, User Support Division, Information Technology and Communication (ITC), University of Virginia, for his assistance in developing MAP1 and MAP2. Ralph Mason provided critical comments which improved the presentation of this article. This work was supported by DARPA/NASA and the Army Research Office.

REFERENCES

1. D. Maurice and T.H. Courtney: *Metall. Mater. Trans. A*, 1994, vol. 25A, pp. 147-158.
2. D. Maurice and T.H. Courtney: *Metall. Mater. Trans. A*, 1995, vol. 26A, pp. 2431-35.
3. J.S. Benjamin and T.E. Volin: *Metall. Trans.*, 1974, vol. 5, pp. 1929-34.
4. R.M. Davis, B. McDermott, and C.C. Koch: *Metall. Trans. A*, 1988, vol. 19A, pp. 2867-74.
5. R.W. Rydin, D. Maurice, and T.H. Courtney: *Metall. Trans. A*, 1993, vol. 24A, pp. 175-85.
6. T.H. Courtney and D.R. Maurice: *Solid State Powder Processing*, A.H. Clauer and J.J. deBarbadillo, eds., TMS, Warrendale, PA, 1989, pp. 1-19.
7. D. Maurice and T.H. Courtney: unpublished Research, 1993.
8. R.B. Schwarz and C.C. Koch: *Appl. Phys. Lett.*, 1987, vol. 50, pp. 1578-87.
9. D.R. Maurice and T.H. Courtney: *Metall. Trans. A*, 1990, vol. 21A, pp. 289-303.
10. A.K. Bhattacharya and E. Arzt: *Scripta Metall. Mater.*, 1992, vol. 27, pp. 749-55.
11. R.J. Comstock, Jr. and T.H. Courtney: *Metall. Mater. Trans. A*, 1994, vol. 25A, pp. 2091-99.
12. P.S. Gilman and W.D. Nix: *Metall. Trans. A*, 1981, vol. 12A, pp. 813-24.
13. D. Maurice and T.H. Courtney: unpublished Research, 1994.
14. *Materials Selector-Materials Engineering*, Special Edition, Reinhold, Stratford, CT, 1991.
15. *The Elsevier Materials Selector*, N.A. Waterman and M.F. Ashby, eds., Elsevier Science, Essex, United Kingdom, and CRC Press, Boca Raton, FL, 1991.
16. *Atlas Of Stress-Strain Curves*, Howard E. Boyer, ed., ASM INTERNATIONAL, Metals Park, OH, 1987.
17. *Metals Handbook*, 9th ed., ASM, Metals Park, OH, 1979, vol. 2.
18. T. Kosmac, D. Maurice, and T.H. Courtney: *J. Am. Ceram. Soc.*, 1992, vol. 76, pp. 2345-52.